



UDC 538.935

EDN VPUHLM

<https://www.doi.org/10.33910/2687-153X-2025-6-2-59-68>

Calcium effect on the Nernst coefficient in double-substituted $Y_{1-x}Ca_xBa_2Cu_{2.8}Zn_{0.2}O_y$

Zh. Xunpeng¹, V. E. Gasumyants ^{1, 2}

¹ Peter the Great St. Petersburg Polytechnic University, 29 Polytechnicheskaya Str.,
Saint Petersburg 195251, Russia

² Herzen State Pedagogical University of Russia, 48 Moika Emb., Saint Petersburg 191186, Russia

Authors

Zhang Xunpeng, ORCID: 0009-0009-7721-5425, e-mail: zhangxunpeng@yandex.com

Vitaliy E. Gasumyants, ORCID: 0000-0002-5306-6738, e-mail: vgasum@yandex.ru

For citation: Xunpeng, Zh., Gasumyants, V. E. (2025) Calcium effect on the Nernst coefficient in double-substituted $Y_{1-x}Ca_xBa_2Cu_{2.8}Zn_{0.2}O_y$. *Physics of Complex Systems*, 6 (2), 59–68. <https://www.doi.org/10.33910/2687-153X-2025-6-2-59-68>
EDN VPUHLM

Received 28 January 2025; reviewed 7 March 2025; accepted 12 March 2025.

Funding: The study did not receive any external funding.

Copyright: © Zh. Xunpeng, V. E. Gasumyants (2025) Published by Herzen State Pedagogical University of Russia. Open access under [CC BY-NC License 4.0](https://creativecommons.org/licenses/by-nc/4.0/).

Abstract. We present experimental results on the temperature dependence of the Nernst coefficient in the normal state of the system $Y_{1-x}Ca_xBa_2Cu_{2.8}Zn_{0.2}O_y$, analyzed quantitatively using a narrow-band model jointly with temperature dependences of the thermopower. From this analysis, we determine the charge carrier mobility across all studied samples and then analyze its variation with increasing calcium content. It is shown that all experimental and calculated results can be explained if we take into account that both calcium and zinc directly affect the structure of the band responsible for the conduction process in the $YBa_2Cu_3O_y$ system. Calcium introduced into the lattice compensates for local disturbances in the electronic structure created by zinc, as a result of which the values of all parameters of the normal state at $x \geq 0.125$ become close to the ones characteristic of undoped $YBa_2Cu_3O_y$.

Keywords: Y-based HTSC, doping, Nernst coefficient, narrow-band model, energy spectrum, charge carrier mobility

Introduction

The unique properties of high-temperature superconductors (HTSCs) have been a major focus of experimental and theoretical research since their discovery in 1987. However, despite extensive studies, the mechanism of electron pairing responsible for the superconductivity phenomenon in these materials remains unclear.

The physics of HTSCs encompasses numerous aspects, many of each offering insights into the unique properties of these materials. In our opinion, the transport properties of HTSC are of undoubted interest for research. As is known, the transport coefficients in the normal state of HTSC exhibit very unusual behavior compared to conventional materials (Gasumyants 2001; Iye 1992; Kaiser, Ucher 1991; Ong 1990), which reflect the unconventional energy spectrum of charge carriers. Although a complete theory of high-temperature superconductivity is still lacking, it is evident that the normal-state parameters of the charge carrier system influence the critical temperature (T_c). For this reason, the information on the nature and the parameters of the normal state is needed for developing the theory that can explain this phenomenon. Such an information can be obtained by studying and analyzing the transport coefficients. The reliable data on the structure of the energy spectrum and the changes in its parameters

under varied sample composition should help to better understand the nature of the normal state in HTSC. Moreover, identifying correlations between the values of these parameters and T_c could indirectly help to verify theoretical models aiming to explain the mechanism of electron pairing in HTSC. This requires determining fundamental HTSC parameters, such as the energy parameters of the band responsible for the conduction process; the charge carrier concentration, mobility, and effective mass, as well as obtaining general knowledge about the peculiarities of the energy spectrum structure in these materials and its transformation when varying the composition of the samples. However, there are not many works devoted to this topic among the numerous studies of HTSC. The most likely reason for this situation is the lack of a holistic approach, which should include not only experimental studies of various transport coefficients for samples of different HTSC systems and various compositions, but also their quantitative analysis within the framework of a unified model, which makes it possible to explain the entire set of experimental data. To substantiate the validity of such a model, it is necessary to carry out systematic studies and analysis of the behavior of transport coefficients in HTSC samples with different types and levels of doping. At the same time, it is important that the model used for such an analysis contains a limited number of physically reasonable parameters and allows one not only to describe the behavior of all the main transport coefficients in HTSC, but also to reliably determine the values of these parameters for samples of different compositions.

In our earlier work, we proposed a phenomenological narrow-band model (Gasumyants et al. 1995) that has since been successfully applied to analyze the thermopower, S , in different HTSCs (Gasumyants 2001; Gasumyants, Martynova 2012; Gasumyants et al. 1995; Elizarova, Gasumyants 2000; Martynova, Gasumyants 2013). This approach enabled us to identify the main characteristics of the energy spectrum in HTSCs, as well as a character and mechanisms of its modification under doping. Subsequent studies (Ageev, Gasumyants 2001; Gasumyants et al. 2005) expanded the model's applicability, demonstrating the possibility of its use for quantitative analysis of temperature dependences of the Nernst coefficient, Q . Unlike other transport coefficients, the Nernst coefficient has received far less attention in HTSCs. Moreover, while numerous studies have examined Q in the vortex phase (e. g., Calzona et al. 1995; Huebener et al. 1991; Qussena et al. 1992), its normal-state behavior remains understudied. A few exceptions explore $Q(T)$ dependences in a narrow temperature range above T_c , where anomalously high values in underdoped cuprates suggest the possible formation of electron pairs at $T > T_c$ (Alexandrov, Zavaritsky 2004; Capan et al. 2002; Tan, Levin 2004; Wang et al. 2001; Xu et al. 2000).

The scarcity of data on Nernst coefficient temperature dependence $Q(T)$ at temperatures well above T_c primarily stems from the lack of suitable analytical methods for studying this behavior in a wide temperature range. Our narrow-band model effectively addresses this challenge. Importantly, this approach enables simultaneous description of four main transport coefficients — resistivity, thermopower, Hall coefficient, and Nernst coefficient (Ageev, Gasumyants 2001; Gasumyants, Martynova 2012). It also allows for joint quantitative analysis of both $S(T)$ and $Q(T)$ dependences (Ageev, Gasumyants 2001; Gasumyants et al. 2005). As shown in (Gasumyants et al. 2005; Gasumyants, Martynova 2018), this methodology additionally provides determination of real charge carrier mobility values.

To study the nature of the normal state, it is necessary to use doped samples with sequentially changing composition and analyze the changes in the found values of model parameters depending on the type and content of the introduced impurity. While numerous cations can substitute into the $YBa_2Cu_3O_y$ lattice (Felner 1991), most impurities exhibit qualitatively similar effects on both superconducting and normal-state transport properties. The most interesting impurity for research in the case of the $YBa_2Cu_3O_y$ system is undoubtedly calcium. Calcium doping produces unusual modifications to transport coefficient temperature dependences and can also enhance superconducting properties if they were previously suppressed by other impurities or oxygen deficiency (Awana et al. 1996; Gasumyants et al. 1994; 2000; Gasumyants, Martynova 2017; Martynova et al. 2011; Suard et al. 1992). In systems like $Y_{1-x}Ca_xBa_2Cu_{2.75}Co_{0.25}O_y$ and $Y_{1-x}Ca_xBa_{1.5}La_{0.5}Cu_3O_y$, the observed T_c enhancement under calcium doping appears linked to its influence on the oxygen subsystem and consequent modifications to the energy spectrum (Gasumyants et al. 1994; 2000; Gasumyants, Martynova 2017). Higher-valence impurities (Co or La) increase oxygen content causing the conductive band broadening, while subsequent calcium doping restores near-stoichiometric oxygen levels, improving subsystem ordering. This influence the energy spectrum parameters in the opposite direction, bringing them closer to those of undoped $YBa_2Cu_3O_y$ and consequently increasing T_c . Interestingly, calcium doping in $Y_{1-x}Ca_xBa_2Cu_{2.8}Zn_{0.2}O_y$ also elevates T_c (Martynova et al. 2011), despite zinc being an isovalent impurity that neither affects oxygen content and suppresses T_c through pair-breaking effect (Bonn et al. 1994; Wang et al. 1998).

Zinc does, however, also modify the normal-state energy spectrum (Gupta, Gupta 1999; Martin, Gasumyants 2021). This circumstance makes the $Y_{1-x}Ca_xBa_2Cu_{2.8}Zn_{0.2}O_y$ system particularly compelling for detailed investigation of calcium's role.

Motivated by these considerations, we present the results of a systematic study of the normal-state Nernst coefficient in the double-substituted $Y_{1-x}Ca_xBa_2Cu_{2.8}Zn_{0.2}O_y$ system across varying calcium concentrations, as well as their quantitative analysis within the narrow-band model framework using previously obtained data for the thermopower behavior in the same samples.

Samples and experimental details

Single-phase ceramic samples of $Y_{1-x}Ca_xBa_2Cu_{2.8}Zn_{0.2}O_y$ ($x = 0.05, 0.1, 0.125, 0.15, 0.175, \text{ and } 0.2$) were synthesized via standard solid-state reaction using high-purity oxide and carbonate precursors. Previous studies (Gasumyants 2001; Gasumyants, Martynova 2017; Martynova et al. 2011) show that oxygen-rich calcium- and zinc-doped samples exhibit transport coefficients with extremely small absolute values, making accurate analysis of their temperature dependences within our model framework challenging. To address this, we performed controlled oxygen reduction through additional vacuum annealing at 460°C for 2 hours. The temperature-dependent resistivity and thermopower data for these samples, along with their thermopower analysis, have been previously reported (Martynova et al. 2011). These datasets will be incorporated in our current analysis and discussion of the Nernst coefficient results. To confirm sample stability over time, we re-measured the thermopower temperature dependences $S(T)$ for two representative samples, obtaining excellent agreement with earlier measurements.

The Nernst coefficient measurements were performed under a constant reversible magnetic field of $B = 1.8$ T. For each temperature, the Nernst signal was measured twice in opposite magnetic field directions and then calculated as the half-difference of the corresponding voltages. This approach effectively eliminates even magnetic effects and significantly improves measurement precision. To increase the signal-to-noise ratio, the sample geometry was optimized to be long (about $l = 10$ mm) in the Nernst signal, U , direction, and thin (about $d = 1$ mm) in the temperature gradient direction. The temperature difference applied to the samples was about $\Delta T = 10$ K. Our measurement protocol was validated through extensive test measurements confirming the linear response regime for HTSCs. The Nernst signal (U) maintains linear dependence on temperature gradient (ΔT) up to $\Delta T = 30\text{--}35$ K, as established in (Gasumyants, Martynova 2018). The Nernst coefficient values were calculated as $Q = U \cdot d / B \cdot \Delta T \cdot l$. The temperature range of measurements was from 100 K to 320 K.

Experimental results

Figure 1 presents the temperature dependences of the Nernst coefficient $Q(T)$ for the investigated samples, excluding the $x = 0.05$ and $x = 0.15$ compositions, the results for which are very close to other experimental curves. As for other doped samples of the $YBa_2Cu_3O_y$ (Gasumyants et al. 2005; Gasumyants, Martynova 2018), the Nernst coefficient has very small values and shows typical changes with temperature. The Nernst coefficient is extremely small near $T = 100$ K, increases sharply with increasing temperature, reaching maximum values in the normal state, and then decreases slightly at temperatures above $T > 150\text{--}200$ K (with the exact transition temperature varying by composition). This conventional behavior shows notable deviations in samples with lower calcium content ($x = 0.05\text{--}0.125$), where the Q values exhibit a pronounced decrease at elevated temperatures beyond the maximum point, as clearly illustrated by the $x = 0.1$ data in Figure 1. This anomalous effect displays a strong calcium concentration dependence, appearing most distinctly in the sample with lowest calcium content and progressively diminishing with its increase until it vanishes completely at calcium content of $x \geq 0.15$.

Figure 2 displays the room-temperature Nernst coefficient ($Q_{300\text{K}}$) as a function of calcium content, compared with corresponding thermopower values ($S_{300\text{K}}$) from previous work (Martynova et al. 2011). While most substitutions in $YBa_2Cu_3O_y$ yield qualitatively similar changes in all transport coefficients (Gasumyants, Martynova 2018), the $Y_{1-x}Ca_xBa_2Cu_{2.8}Zn_{0.2}O_y$ system exhibits distinct behavior. The thermopower shows a consistent monotonic decrease with increasing x , whereas the Nernst coefficient displays a more complex dependence: $Q_{300\text{K}}$ decreases for $x = 0\text{--}0.125$, but rises at higher calcium concentrations. This contrasts with the monotonic $Q_{300\text{K}}$ variation observed in the case of single calcium doping (Gasumyants, Martynova 2018).

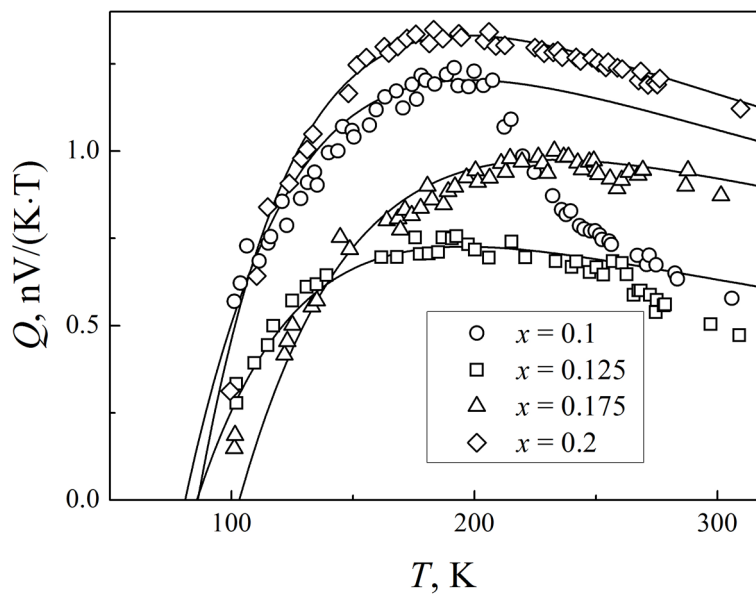


Fig. 1. Temperature dependences of the Nernst coefficient in $Y_{1-x}Ca_xBa_2Cu_{2.8}Zn_{0.2}O_y$. Symbols indicate experimental results; lines indicate the results of calculation within the narrow-band model

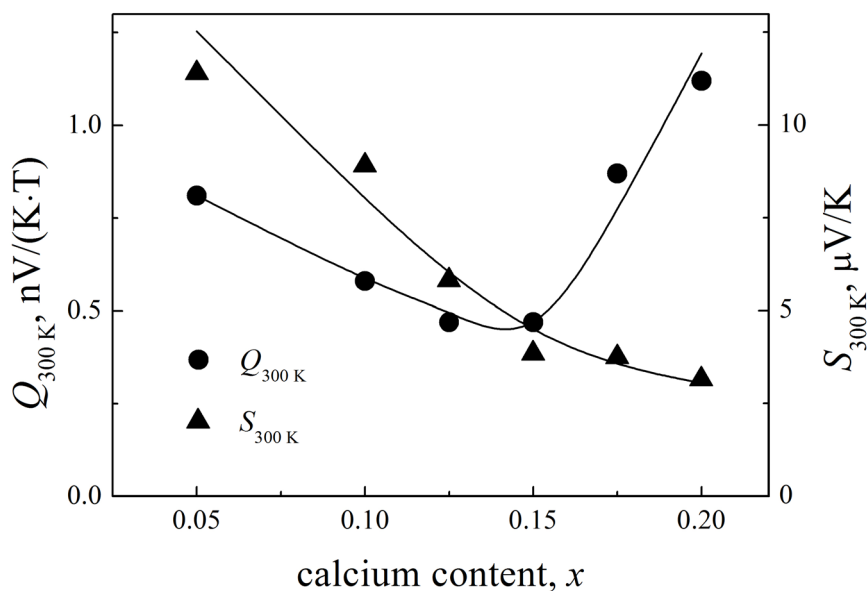


Fig. 2. Room-temperature Nernst coefficient and thermopower in $Y_{1-x}Ca_xBa_2Cu_{2.8}Zn_{0.2}O_y$

The observed evolution of $Q(T)$ behavior with increasing calcium content in $Y_{1-x}Ca_xBa_2Cu_{2.8}Zn_{0.2}O_y$ likely stems from the influences of zinc and calcium on the conduction band structure. Zinc substitutes for plane copper, which participates directly in conduction band formation, and according to the results presented in (Gupta, Gupta 1999), removes electronic states from this band destroying its structure, as confirmed by our thermopower analysis in $YBa_2Cu_{3-x}Zn_xO_y$ (Martin, Gasumyants 2021). This substitution also significantly perturbs the system’s electronic structure (Gupta, Gupta 1999), particularly affecting charge carrier scattering. The Nernst coefficient’s enhanced sensitivity to scattering processes explains why the $YBa_2Cu_{3-x}Zn_xO_y$ system with substantial zinc content maintains conventional $S(T)$ behavior while developing anomalous features in $Q(T)$, as observed in our measurements. Conversely, calcium doping introduces additional states into the conduction band (Gasumyants, Martynova 2017), effectively counteracting zinc-induced modifications in the $Y_{1-x}Ca_xBa_2Cu_{2.8}Zn_{0.2}O_y$ system. This compensation mechanism accounts for the monotonic decrease in $S_{300 K}$ with increasing x (Fig. 2) and the systematic evolution

of energy spectrum parameters, the values of which at calcium content $x \geq 0.15$ approach those characteristic of undoped $\text{YBa}_2\text{Cu}_3\text{O}_y$, as revealed by our $S(T)$ analysis (Martynova et al. 2011).

Contrary to the thermopower, the Nernst coefficient behavior is affected by disruptions of the electronic structure induced by zinc. At low calcium contents in the $\text{Y}_{1-x}\text{Ca}_x\text{Ba}_2\text{Cu}_{2.8}\text{Zn}_{0.2}\text{O}_y$ system ($x < 0.15$), it gradually compensates for the effect of zinc on the energy spectrum structure. This results in a drop in the $Q_{300\text{K}}$ value and a decrease in the degree of deviation of the $Q(T)$ dependences from the typical form. This compensation becomes nearly complete at $x \geq 0.15$. As a result, the $Q(T)$ dependences take on a typical form, and the $Q_{300\text{K}}$ value increases with increasing x , as in the case of single calcium doping in the $\text{YBa}_2\text{Cu}_3\text{O}_y$ system.

Note that our conclusion regarding calcium's compensating effect on zinc-induced modifications in the normal-state energy spectrum in $\text{YBa}_2\text{Cu}_3\text{O}_y$ is further supported by recent studies of the $\text{Y}_{1-x}\text{Ca}_x\text{Ba}_2\text{Cu}_{3-x}\text{Zn}_x\text{O}_y$ system with equal content of two dopants (Funtikova, Gasumyants 2023), which revealed very slight changes in the energy spectrum parameters over a wide range of doping levels. Thus, it is the compensating effect of calcium that causes the modification of the $Q(T)$ dependences described above, as well as the observed $Q_{300\text{K}}(x)$ dependence in the $\text{Y}_{1-x}\text{Ca}_x\text{Ba}_2\text{Cu}_{2.8}\text{Zn}_{0.2}\text{O}_y$ system.

Analysis of experimental results within the narrow-band model and discussion

Our analysis is based on a narrow-band model that assumes the band responsible for the conduction process in HTSCs has a half-width comparable in order of magnitude to the Fermi smearing, with the Fermi level located within this band. Under these conditions, we can approximate density-of-states, $D(E)$, conductivity, $\sigma(E)$, and Hall conductivity, $\sigma_H(E)$, functions by rectangles of different widths (Gasumyants 2001; Gasumyants et al. 1995). This simplification allows us to derive analytical expressions for the thermopower and Nernst coefficient by solving the Boltzmann transport equation within the relaxation time approximation (Ageev, Gasumyants 2001; Gasumyants et al. 1995):

$$S = -\frac{k_B}{e} \left\{ \frac{W_\sigma^*}{\sinh W_\sigma^*} \left[\exp(-\mu^*) + \cosh W_\sigma^* - \frac{1}{W_\sigma^*} (\cosh \mu^* + \cosh W_\sigma^*) \times \right. \right. \\ \left. \left. \times \ln \frac{\exp(\mu^*) + \exp(W_\sigma^*)}{\exp(\mu^*) + \exp(-W_\sigma^*)} \right] - \mu^* \right\}, \quad (1)$$

$$Q = \frac{1}{eT} u \left(\frac{I_{H_1}}{I_0} - \frac{I_{H_0} I_1}{I_0^2} \right), \quad (2)$$

where

$$I_i = \int_{-W_\sigma/2+bW_D}^{W_\sigma/2+bW_D} \left(-\frac{\partial f_0}{\partial E} \right) E^i dE, \quad I_{H_i} = \int_{-W_\sigma/2+kW_D}^{W_\sigma/2+kW_D} \left(-\frac{\partial f_0}{\partial E} \right) \text{sign}(E - kW_D) E^i dE,$$

k_B is the Boltzmann constant, e is the elementary charge, f_0 is the equilibrium Fermi-Dirac distribution function, $\mu^* \equiv \mu/k_B T = \ln \frac{\sinh(FW_D^*)}{\sinh[(1-F)W_D^*]} - 2bW_D^*$, $W_\sigma^* \equiv W_\sigma/2k_B T$, $W_D^* \equiv W_D/2k_B T$, μ is the electrochemical potential measured from the middle of the band. As is seen, the $S(T)$ dependence is determined by four physically significant model parameters, namely, the degree of band filling with electrons F , representing the ratio of the total number of electrons to the total number of states in the band; the total effective bandwidth W_D ; the effective width of the delocalized state interval W_σ ; and the band asymmetry degree b . The latter three parameters are introduced into the model as describing the approximations we use. The W_D and W_σ values are the widths of rectangles approximating the functions $D(E)$ or $\sigma(E)$ and $\sigma_H(E)$, respectively, as a result their ratio $C \equiv W_\sigma/W_D$ characterizes the degree of delocalization of charge carriers at the band edges. The b value determines the energy shift bW_D between the centers of these rectangles, which arises due to the possible asymmetry of the density-of-state function.

The calculation of the Nernst coefficient's temperature dependence $Q(T)$ requires the introduction of two additional parameters. They are the band-averaged electron mobility u , and the dispersion law asymmetry parameter k , which determines the energy shift kW_D of the sign-change point in the Hall conductivity $\sigma_H(E)$ function relative to the band center. Since Eq. (2) shows that $Q(T)$ depends

collectively on all six model parameters, its independent analysis is not feasible. To apply the described approach, it is necessary to measure both the $S(T)$ and $Q(T)$ dependences on the same samples and then analyze them together. In such a case, the four primary parameters are first determined through thermopower analysis using Eq. (1). These values are then used in Eq. (2) to extract the two remaining parameters from Nernst coefficient analysis (Ageev, Gasumyants 2001; Gasumyants et al. 2005). As demonstrated in previous studies (Gasumyants et al. 2005; Gasumyants, Martynova 2018), this joint analysis of thermopower and Nernst coefficient data enables unambiguous determination of all model parameters in doped $YBa_2Cu_3O_y$ systems.

Figure 3 presents the experimental thermopower data $S(T)$ for the $Y_{1-x}Ca_xBa_2Cu_{2.8}Zn_{0.2}O_y$ system (Martynova et al. 2011), along with best-fitted curves calculated using Eq. (1). The corresponding calculated $Q(T)$ dependences from Eq. (2) are shown in Figure 1. One can see that the narrow-band model allows us to well describe the temperature dependences of both transport coefficients using a single set of model parameters. Two aspects of the fitting procedure deserve mention. First, for samples with low calcium content, we restricted the $Q(T)$ fitting to the low-temperature regime, intentionally excluding the high-temperature region where zinc-induced perturbations of the electronic structure cause anomalous suppression of the Nernst coefficient (as discussed previously). Second, since in the case of an asymmetric band we need to use four parameters to calculate the $S(T)$ dependence, their values can be determined with some errors. The simultaneous fitting of both $S(T)$ and $Q(T)$ data not only determines the u and k parameters, but also enables refinement of the initial parameter estimates, yielding optimal agreement between the experimental and calculated curves for the two studied coefficients.

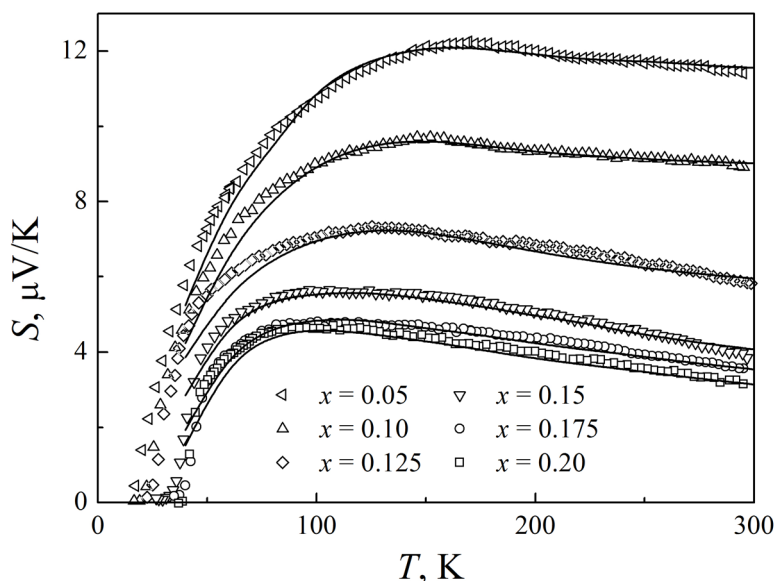


Fig. 3. Temperature dependences of the thermopower in $Y_{1-x}Ca_xBa_2Cu_{2.8}Zn_{0.2}O_y$. Symbols indicate experimental results; lines indicate results of calculation within the narrow-band model

The complete set of model parameters characterizing calcium's influence on the electronic structure and charge carrier system in $Y_{1-x}Ca_xBa_2Cu_{2.8}Zn_{0.2}O_y$ is presented in Table 1. The detailed discussion of calcium-induced changes in the F , W_D , W_σ , and b parameters, as well as the physical reasons for these changes, can be found elsewhere (Martynova et al. 2011). Here we would only like to emphasize that the energy parameters of the band (W_D and W_σ), which are little affected by zinc introduction, remain almost constant for all the studied samples. The band filling degree F and asymmetry parameter b exhibit systematic evolution with calcium content, progressively approaching the characteristic values of an undoped sample ($F \approx 0.5$, $b \approx 0$), while in calcium-free $YBa_2Cu_{2.8}Zn_{0.2}O_y$ they differ significantly from these values due to the zinc effect. This behavior quantitatively confirms calcium's compensating effect on zinc-induced electronic structure modifications, as discussed above.

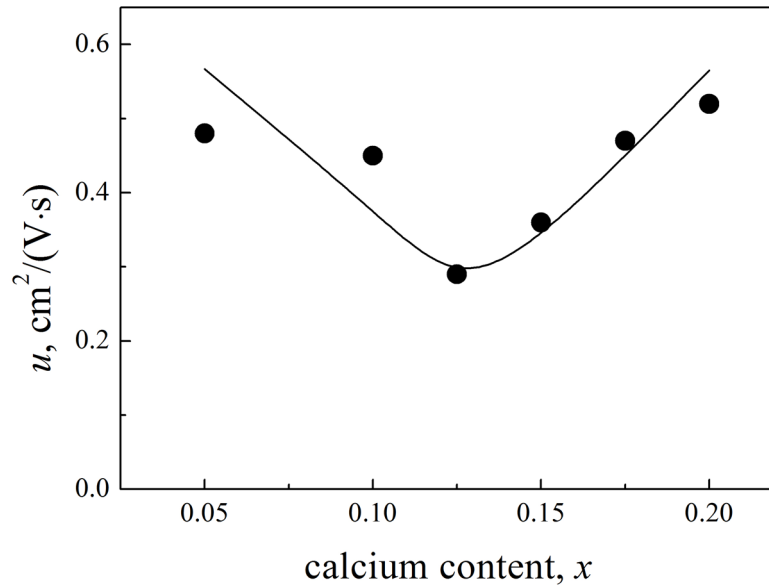
Figure 4 presents the calculated charge carrier mobility values, which represent the band-averaged mobility determined through our narrow-band model rather than the conventional Nernst mobility defined as $Q/(k_B/e)$. This explains why the $u(x)$ dependence differs from the $Q_{300K}(x)$ behavior shown in Figure 2. The obtained mobility values are characteristically small, less than $1 \text{ cm}^2/(\text{V}\cdot\text{s})$, which

Table 1. The values of model parameters determined from the joint analysis of the $S(T)$ and $Q(T)$ dependences in the $Y_{1-x}Ca_xBa_2Cu_{2.8}Zn_{0.2}O_y$ system

x	F	W_D, meV	$C \equiv W_\sigma / W_D$	b	$u, \text{cm}^2/(\text{V}\cdot\text{s})$	k	$k \cdot W_D, \text{meV}$
0.05	0.535	102	0.37	0.017	0.48	-0.11	-11.2
0.1	0.524	96	0.36	0.011	0.45	-0.12	-11.5
0.125	0.520	103	0.39	0.007	0.29	-0.13	-13.4
0.15	0.517	97	0.33	0.004	0.36	-0.12	-11.6
0.175	0.513	95	0.35	0.000	0.47	-0.15	-14.3
0.2	0.509	90	0.41	-0.002	0.52	-0.15	-13.5

is consistent with previous results obtained for samples of the $YBa_2Cu_3O_y$ system with various types and levels of substitutions (Gasumyants, Martynova 2018). The mobility exhibits a non-monotonic dependence on calcium content, initially decreasing before showing an increase beyond $x = 0.125$. Note that to explain the variations in the mobility value under increasing doping level in various Y-based HTSC systems, we usually considered corresponding changes in the W_D and $C \equiv W_\sigma / W_D$ values (Gasumyants, Martynova 2018). As shown earlier (Gasumyants 2001), in most doped $YBa_2Cu_3O_y$ systems, non-isovalent impurities typically cause band broadening (increased W_D) and enhanced state localization at band edges (decreased $C \equiv W_\sigma / W_D$) via Anderson localization mechanism (Anderson 1958). Calcium doping in pre-doped systems produces the opposite effect on both these parameters (Gasumyants et al. 2000; Gasumyants, Martynova 2017).

The charge carrier mobility, defined as $u = e\langle\tau\rangle/m^*$, where $\langle\tau\rangle$ is the averaged relaxation time and m^* is the effective mass of electrons, exhibits doping-dependent behavior governed by two competing factors. Band broadening typically reduces the effective mass, which would enhance mobility, while impurity-induced disorder increases charge carrier scattering, reducing the relaxation time and consequently decreasing mobility. By analyzing these competing effects, we can consistently explain the doping-dependent mobility evolution observed in various doped systems (Gasumyants, Martynova 2018).

Fig. 4. Calculated charge-carrier mobility for $Y_{1-x}Ca_xBa_2Cu_{2.8}Zn_{0.2}O_y$ samples

Clearly, this approach cannot be applied to analyze the $u(x)$ dependence in the studied $Y_{1-x}Ca_xBa_2Cu_{2.8}Zn_{0.2}O_y$ system. As Table 1 shows, both the W_D and C values exhibit only minimal variation with increasing calcium content. However, it is important to note that W_D and W_σ represent effective widths of their respective energy intervals, namely the widths of rectangles approximating the $D(E)$ and $\sigma(E)$ functions. Most

substitutions in the $YBa_2Cu_3O_y$ system affect the energy spectrum indirectly through band broadening caused by the Anderson localization mechanism (Gasumyants 2001). In such cases, changes in W_D and W_σ accurately reflect the actual modifications of the $D(E)$ and $\sigma(E)$ functions under doping. In contrast, both calcium and zinc directly modify the energy spectrum — either through the formation of an additional Ca-induced peak in the $D(E)$ function or via Zn-induced state removal from the band. Under these circumstances, the rectangular approximation becomes too crude to quantitatively explain mobility variations by considering changes in the above two parameters. Qualitatively, the observed $u(x)$ dependence in $Y_{1-x}Ca_xBa_2Cu_{2.8}Zn_{0.2}O_y$ can be understood as follows. At low doping levels, calcium partially compensates for zinc's effect on the energy spectrum while simultaneously introducing additional disorder to the electronic structure established by zinc incorporation, ultimately reducing mobility. Near $x \approx 0.125$, zinc's influence becomes nearly compensated, as evidenced by the shape of the $Q(T)$ dependence for samples with $x \geq 0.15$ (discussed earlier). Further calcium doping, once zinc compensation is complete, increases mobility, which is consistent with previous observations in oxygen-deficient $Y_{1-x}Ca_xBa_2Cu_3O_y$ systems (Gasumyants, Martynova 2018). Thus, the change in the charge-carrier mobility in $Y_{1-x}Ca_xBa_2Cu_{2.8}Zn_{0.2}O_y$ with increasing calcium content can be explained by taking into account the compensating effect of calcium, similar to the explanation of the experimental results on the behavior of the Nernst coefficient.

As shown in Table 1, the dispersion law asymmetry parameter k remains negative and varies only slightly with changes of calcium content x in the $Y_{1-x}Ca_xBa_2Cu_{2.8}Zn_{0.2}O_y$ system. The kW_D value, representing the energy shift of the Hall conductivity sign-change point relative to the band center, also changes slightly between 11 and 14 meV. Note that this dispersion law asymmetry is not directly related to the asymmetry of the $D(E)$ function (parameter b in Table 1), which changes quite strongly in the studied system due to calcium-induced states appearing within the band. Our earlier studies (Gasumyants, Martynova 2018) established that such dispersion law asymmetry constitutes an intrinsic feature of the $YBa_2Cu_3O_y$ electronic structure, whereas the band asymmetry b emerges only under specific types of doping. Notably, despite the W_D value changes quite strongly with certain types of doping, the kW_D value in all cases varies in a relatively narrow range (Gasumyants, Martynova 2018). In particular, this value changes by 3 or 5 meV in cases of single doping with calcium or zinc, respectively, when the content of corresponding dopant changes from $x = 0$ to $x = 0.2$. The present results for double-substituted $Y_{1-x}Ca_xBa_2Cu_{2.8}Zn_{0.2}O_y$ system thus align well with this established pattern.

Conclusions

We have experimentally studied the Nernst coefficient in the $Y_{1-x}Ca_xBa_2Cu_{2.8}Zn_{0.2}O_y$ system with varying calcium content in the normal state and analyzed the $Q(T)$ dependences together with the thermopower data. The main results are as follows.

For samples with low calcium content ($x \leq 0.125$), the Nernst coefficient at high temperatures deviates from the temperature dependence characteristic of doped $YBa_2Cu_3O_y$ samples. This deviation gradually diminishes with increasing calcium content and vanishes completely for $x \geq 0.15$. Across all compositions, the room-temperature Nernst coefficient remains below 1 nV/(K·T), showing slight but non-monotonic variation with doping level. The behavior of both thermopower and Nernst coefficient in $Y_{1-x}Ca_xBa_2Cu_{2.8}Zn_{0.2}O_y$ can be satisfactorily described and quantitatively analyzed using the narrow-band model. This joint analysis allows one to determine, besides the fundamental energy spectrum parameters, the values of the charge-carrier mobility and the degree of dispersion law asymmetry. Despite calcium doping systematically modifies the density-of-states asymmetry, the dispersion law asymmetry remains essentially constant. This demonstrates that the latter represents an intrinsic feature of the $YBa_2Cu_3O_y$ energy spectrum rather than being doping-specific. The charge carrier mobility, which is notably low in all samples, decreases with an increase in calcium content at low doping levels, but increases for $x \geq 0.125$. These mobility variations, along with the Nernst coefficient behavior and changes in the calculated parameters of the energy spectrum structure, can be qualitatively explained by the compensating effect of calcium on zinc-induced disturbances in the electronic structure of the conductive band. Consequently, calcium doping enhances both superconducting properties and normal-state charge carrier characteristics in the $Y_{1-x}Ca_xBa_2Cu_{2.8}Zn_{0.2}O_y$ system.

Conflict of Interest

The authors declare that there is no conflict of interest, either existing or potential.

Author Contributions

Zh. Xunpeng performed measurements and simulations of Nernst coefficient temperature dependences and wrote the manuscript; V. E. Gasumyants analyzed the results and wrote the manuscript.

References

- Ageev, N. V., Gasumyants, V. E. (2001) The Nernst-Ettingshausen coefficient in conductors with a narrow conduction band: Analysis and application of its results to HTSC materials. *Physics of the Solid State*, 43, 1834–1844. <https://doi.org/10.1134/1.1410619> (In English)
- Alexandrov, A. S., Zavaritsky, N. V. (2004) Nernst effect in poor conductors and in the cuprate superconductors. *Physical Review Letters*, 93, article 217002. <https://doi.org/10.1103/PhysRevLett.93.217002> (In English)
- Anderson, P. W. (1958) Absence of diffusion in certain random lattices. *Physical Review*, 109, 1492–1505. <https://doi.org/10.1103/PhysRev.109.1492> (In English)
- Awana, V. P. S., Malik, S. K., Yelon, W. B. (1996) Structural aspects and superconductivity in oxygen-deficient $Y_{1-x}Ca_xBa_2Cu_3O_{7-y}$ ($y \approx 0.3$) systems: A neutron-diffraction study. *Physica C: Superconductivity*, 262 (3–4), 272–278. [https://doi.org/10.1016/0921-4534\(96\)00213-4](https://doi.org/10.1016/0921-4534(96)00213-4) (In English)
- Bonn, D. A., Kamal, S., Zhang, K., et al. (1994) Comparison of the influence of Ni and Zn impurities on the electromagnetic properties of $YBa_2Cu_3O_{6.95}$. *Physical Review B*, 50, 4051–4063. <https://doi.org/10.1103/PhysRevB.50.4051> (In English)
- Calzona, V., Cimberle, M. R., Ferdeghini, C. et al. (1995) Thermoelectric and thermomagnetic effects in the mixed state analysis of the thermal angle. *Physica C: Superconductivity*, 246, 169–176. [https://doi.org/10.1016/0921-4534\(95\)00124-7](https://doi.org/10.1016/0921-4534(95)00124-7) (In English)
- Capan, C., Behnia, K., Hinderer, J. et al. (2002) Entropy of vortex cores near the superconductor-insulator transition in an underdoped cuprate. *Physical Review Letters*, 88, article 056601. <https://doi.org/10.1103/PhysRevLett.88.056601> (In English)
- Elizarova, M. V., Gasumyants, V. E. (2000) Band spectrum transformation and T_c variation in the $La_{2-x}Sr_xCuO_y$ system in the underdoped and overdoped regimes. *Physical Review B*, 62, 5989–5996. <https://doi.org/10.1103/PhysRevB.62.5989> (in English)
- Felner, I. (1991) The effect of chemical substitution on superconductivity in $YBa_2Cu_3O_7$. *Thermochimica Acta*, 174, 41–69. [https://doi.org/10.1016/0040-6031\(91\)80152-9](https://doi.org/10.1016/0040-6031(91)80152-9) (In English)
- Funtikova, A., Gasumyants, V. (2023) Experimental study and analysis of the thermopower in the $Y_{1-x}Ca_xBa_2Cu_{3-x}Zn_xO_y$ system. In: *Proceedings of the 2023 International Conference on Electrical Engineering and Photonics (EExPolytech)*. [S. l.]: IEEE Publ., pp. 300–303. <https://doi.org/10.1109/EExPolytech58658.2023.10318628> (In English)
- Gasumyants, V. E. (2001) Analysis of the electron transport phenomena in HTSC-materials as the method of studying the band spectrum and its transformation under doping by different impurities. In: F. Gerard (ed.). *Advances in Condensed Matter and Materials Research. Vol. 1*. New York: Nova Science Publ., pp. 135–200. (In English)
- Gasumyants, V. E., Elizarova, M. V., Vladimirskaya, E. V., Patrino, I. B. (2000) Ca effect on the normal-state and superconducting properties of Y-based HTS. *Physica C: Superconductivity*, 341–348, 585–588. [https://doi.org/10.1016/S0921-4534\(00\)00604-3](https://doi.org/10.1016/S0921-4534(00)00604-3) (In English)
- Gasumyants, V. E., Ageev, N. V., Elizarova, M. V. (2005) The Nernst-Ettingshausen coefficient in the normal phase of doped HTSCs of the $YBa_2Cu_3O_y$ system. *Physics of the Solid State*, 47, 202–213. <https://doi.org/10.1134/1.1866394> (In English)
- Gasumyants, V. E., Kaidanov, V. I., Vladimirskaya, E. V. (1995) The electron transport phenomena in Y-based HTSC's and their analysis on the basis of phenomenological narrow-band theory. The band structure transformation with oxygen content and substitution for Cu. *Physica C: Superconductivity*, 248, 255–275. [https://doi.org/10.1016/0921-4534\(95\)00173-5](https://doi.org/10.1016/0921-4534(95)00173-5) (In English)
- Gasumyants, V. E., Martynova, O. A. (2012) Normal-state band spectrum in chain-free high-temperature superconductors: mechanisms of modification under changing sample composition and influence of the normal-state parameters on the critical temperature. In: V. Rem Romanovskii (ed.). *Superconductivity: Theory, Materials and Applications*. New York: Nova Science Publ., pp. 285–326. (In English)
- Gasumyants, V. E., Martynova, O. A. (2017) Specific features of the thermopower behavior of calcium-containing Y-based high-temperature superconductors: Experimental investigation and interpretation. In: A. Reimer (ed.). *Horizons in World Physics. Vol. 291*. New York: Nova Science Publ., pp. 129–216. (In English)
- Gasumyants, V. E., Martynova, O. A. (2018) Experimental investigation and quantitative analysis of the normal-state Nernst coefficient in doped high-temperature superconductors of the $YBa_2Cu_3O_y$ system. In: M. Miryala, M. R. Koblishka (eds.). *High-Temperature Superconductors: Occurrence, Synthesis and Applications*. New York: Nova Science Publ., pp. 95–152. (In English)

- Gasumyants, V. E., Vladimirskaia, E. V., Patrino, I. B. (1994) Transport properties, band spectrum, and superconductivity in the $Y_{1-x}Ca_xBa_2Cu_{3-z}Co_zO_y$ system. *Physica C: Superconductivity*, 235–240, 1467–1468. [https://doi.org/10.1016/0921-4534\(94\)91958-5](https://doi.org/10.1016/0921-4534(94)91958-5) (In English)
- Gupta, R. P., Gupta, M. (1999) Effect of nickel and zinc substitutions on the electronic charge-density redistribution in a $YBa_2Cu_3O_7$ superconductor. *Physical Review B*, 59, 3381–3384. <https://doi.org/10.1103/PhysRevB.59.3381> (In English)
- Huebener, R. P., Kober, F., Ri, H.-C. et al. (1991) Seebeck and Nernst effect in the mixed state of slightly oxygen deficient $YBaCuO$. *Physica C: Superconductivity*, 181, 345–354. [https://doi.org/10.1016/0921-4534\(91\)90122-F](https://doi.org/10.1016/0921-4534(91)90122-F) (In English)
- Iye, Y. (1992) Transport properties of high T_c cuprates. In: D. M. Ginsberg (ed.). *Physical Properties of High Temperature Superconductors III*. Singapore: World Scientific Publ., pp. 285–361. (In English)
- Kaiser, A. B., Ucher, C. (1991) Thermoelectricity of high-temperature superconductors. In: A. V. Narlikar (ed.). *Studies of High Temperature Superconductors. Vol. 7*. New York: Nova Science Publ., pp. 353–392. (In English)
- Martin, E., Gasumyants, V. (2021) Zinc doping effect on the thermopower behavior and the modification of the normal-state energy spectrum in the $YBa_2Cu_3O_y$ system. In: *Proceedings of the 2021 International Conference on Electrical Engineering and Photonics (EExPolytech)*. [S. l.]: IEEE Publ., pp. 153–156. <https://doi.org/10.1109/EExPolytech53083.2021.9614800> (In English)
- Martynova, O. A., Potapov, D. V., Gasumyants, V. E., Vladimirskaia, E. V. (2011) Mechanism of a strong rise of T_c due to the calcium doping in $Y_{1-x}Ca_xBa_2Cu_{2.8}Zn_{0.2}O_y$. *Physica C: Superconductivity*, 471, 308–313. <https://doi.org/10.1016/j.physc.2011.02.011> (In English)
- Martynova, O. A., Gasumyants, V. E. (2013) Mechanism of cerium doping-induced formation and modification of the energy spectrum in the $Nd_{2-x}Ce_xCuO_y$ system. *Physics of the Solid State*, 55, 254–261. <https://doi.org/10.1134/S1063783413020200> (In English)
- Ong, N. P. (1990) The Hall effect and its relation to other transport phenomena in the normal state of the high-temperature superconductors. In: D. M. Ginsberg (ed.). *Physical Properties of High Temperature Superconductors II*. Singapore: World Scientific Publ., pp. 459–507. (In English)
- Qussena, M., Gagnon, R., Wang, Y., Aubin, M. (1992) Magneto-Seebeck and Nernst-effect measurements on $YBa_2Cu_3O_{7-x}$ single crystals. *Physical Review B*, 46, 528–531. <https://doi.org/10.1103/PhysRevB.46.528> (In English)
- Suard, E., Maignan, A., Caignaert, V., Raveau, B. (1992) Effect of Y-Ca substitution upon superconductivity in the oxide $YBa_2Cu_{3-x}Co_xO_{7-\delta}$. *Physica C: Superconductivity*, 200, 43–49. [https://doi.org/10.1016/0921-4534\(92\)90320-C](https://doi.org/10.1016/0921-4534(92)90320-C) (In English)
- Tan, S., Levin, K. (2004) Nernst effect and anomalous transport in cuprates: A preformed-pair alternative to the vortex scenario. *Physical Review B*, 69, article 064510. <https://doi.org/10.1103/PhysRevB.69.064510> (In English)
- Wang, N. L., Tajima, S., Rykov, A. I., Tomimoto, K. (1998) Zn-substitution effects on the optical conductivity in $YBa_2Cu_3O_{7-\delta}$ crystals: Strong pair breaking and reduction of in-plane anisotropy. *Physical Review B*, 57, R11081–R11084. <https://doi.org/10.1103/PhysRevB.57.R11081> (In English)
- Wang, Y., Xu, Z. A., Kakeshita, T. et al. (2001) Onset of the vortex-like Nernst signal above T_c in $La_{2-x}Sr_xCuO_4$ and $Bi_2Sr_{2-y}La_yCuO_6$. *Physical Review B*, 64, article 224519. <https://doi.org/10.1103/PhysRevB.64.224519> (In English)
- Xu, Z. A., Ong, N. P., Wang, Y. et al. (2000) Vortex-like excitations and the onset of superconducting phase fluctuation in underdoped $La_{2-x}Sr_xCuO_4$. *Nature*, 406, 486–488. <https://doi.org/10.1038/35020016> (In English)